Data-Driven Maintenance Decision Analytics Using Multimodal Structural Health Indicators for Composite Asset Fleets

Yisong Chen[1], Chuanhao Nie[1,*], Yexin Tian[1]

[1] College of Computing, Georgia Institute of Technology, Atlanta, GA, USA 30332

* Email: cnie30@gatech.edu (Corresponding Author)

Received 19 January 2026 · Revised 5 March 2026 · Accepted 19 April 2026 · Published 30 September 2026

Abstract

The safety, airworthiness, and lifecycle cost efficiency of composite asset fleets depend critically on the ability to derive reliable, interpretable health indicators (HIs) that integrate heterogeneous sensing modalities. Traditional single-modal approaches based on acoustic emission (AE) or guided-wave (GW) interrogation alone suffer from limited representativeness, poor generalization across fleet units, and insufficient monotonicity under stochastic damage accumulation. This study presents a comprehensive data-driven maintenance decision analytics framework that constructs multimodal structural health indicators (SHIs) by fusing passive acoustic emission signals and active guided-wave damage indices. The framework encompasses four integrated layers: multimodal data acquisition and synchronization, modality-specific feature engineering, semi-supervised inter-modality fusion, and fleet-level maintenance decision analytics. Prognostic quality criteria—including monotonicity (Mo), prognosability (Pr), and trendability (Tr)—are embedded directly into the learning objectives to yield health trajectories suitable for remaining useful life (RUL) estimation and maintenance scheduling. Experimental results on a composite panel fatigue dataset demonstrate that the proposed multimodal SHI achieves composite prognostic scores exceeding 0.88, substantially outperforming single-modal baselines. Fleet-level decision analytics translates SHI outputs into condition-based maintenance triggers, demonstrating a 23.4% reduction in unplanned downtime relative to fixed-interval scheduling. The findings underscore the practical value of multimodal fusion for industrial prognostics and health management (PHM) of composite structures.

Keywords: Composite structures; data-driven analytics; structural health monitoring; multimodal sensor fusion; prognostics and health management; maintenance decision analytics; health indicators; remaining useful life

Data-Driven Maintenance Decision Analytics Using Multimodal Structural Health Indicators for Composite Asset Fleets

1. Introduction

Composite materials—including carbon-fibre-reinforced polymers (CFRP) and glass-fibre-reinforced polymers (GFRP)—have become ubiquitous in aerospace, civil aviation, wind energy, and marine structures owing to their exceptional specific strength, stiffness, and corrosion resistance [1, 2]. The transition from metallic to composite primary structures, however, fundamentally alters the failure taxonomy: interlaminar delamination, matrix cracking, fibre fracture, and disbonding evolve concurrently and interact nonlinearly, rendering damage trajectory prediction far more challenging than for isotropic metals [3, 4].

Prognostics and health management (PHM) provides the operational framework for transitioning from time-based maintenance, which relies on conservative fixed intervals, to condition-based maintenance (CBM) and predictive maintenance (PdM), which schedule interventions based on measured health state [5, 6]. Central to this paradigm is the health indicator (HI)—a scalar trajectory that compresses heterogeneous sensor streams into a monotonically evolving degradation index and provides a basis for remaining useful life (RUL) prediction [7, 8]. For composite asset fleets operating under diverse loading spectra, environmental conditions, and usage profiles, the construction of fleet-generalisable HIs that satisfy formal prognostic quality criteria remains an open research challenge [9, 10].

Structural health monitoring (SHM) of composite structures conventionally employs passive sensing, such as acoustic emission (AE), or active sensing, such as piezoelectric-actuated guided waves (GW). AE monitoring captures transient elastic waves emitted during microcrack propagation, fibre pull-out, and delamination events, providing high temporal resolution at the cost of limited spatial localisation [11]. GW interrogation, by contrast, injects Lamb wave pulses that interact with structural discontinuities and reflect damage-induced impedance changes, enabling quantitative damage index (DI) maps with strong spatial resolution at relatively low temporal sampling rates [12, 13]. Neither modality alone encapsulates the full degradation dynamics of composite laminates under fatigue loading, which motivates multimodal fusion strategies [14, 15].

Despite growing interest in sensor fusion for PHM, most published work addresses single-material, single-failure-mode scenarios with limited fleet generalisation. Moreover, ground-truth HI labels are seldom available, creating a supervised learning bottleneck. The integration of data-driven analytics with formal prognostic criteria—monotonicity, prognosability, and trendability—into the fusion objective remains underexplored, particularly for multi-unit fleet assessment [16, 17]. Fleet-level maintenance decision analytics, which translate SHI outputs into actionable maintenance scheduling for heterogeneous asset populations, represent a further gap between academic HI research and industrial deployment [18, 19].

This paper addresses these gaps through a four-layer data-driven framework that fuses AE and GW data streams to construct multimodal SHIs for composite panel fleets and couples the SHI outputs with a fleet-level maintenance decision analytics module. The primary contributions are: (1) a modality-specific feature engineering pipeline with criteria-guided semi-supervised HI construction; (2) a late-fusion meta-learner for inter-modality SHI synthesis; (3) a quantitative comparison of single-modal and multimodal HI quality across standard prognostic metrics; and (4) a fleet-level decision analytics layer that demonstrates practical CBM scheduling improvement. The remainder of this paper is organized as follows. Section 2 reviews the relevant literature. Section 3 describes the proposed framework. Section 4 details the experimental setup and dataset. Section 5 presents results and analysis. Section 6 concludes with key findings and directions for future research.

Figure 1 provides an overview of the proposed four-layer framework, illustrating the data flow from raw sensor acquisition through modality-specific processing, inter-modality fusion, and finally to maintenance decision generation. Each layer is described in detail in Section 3.

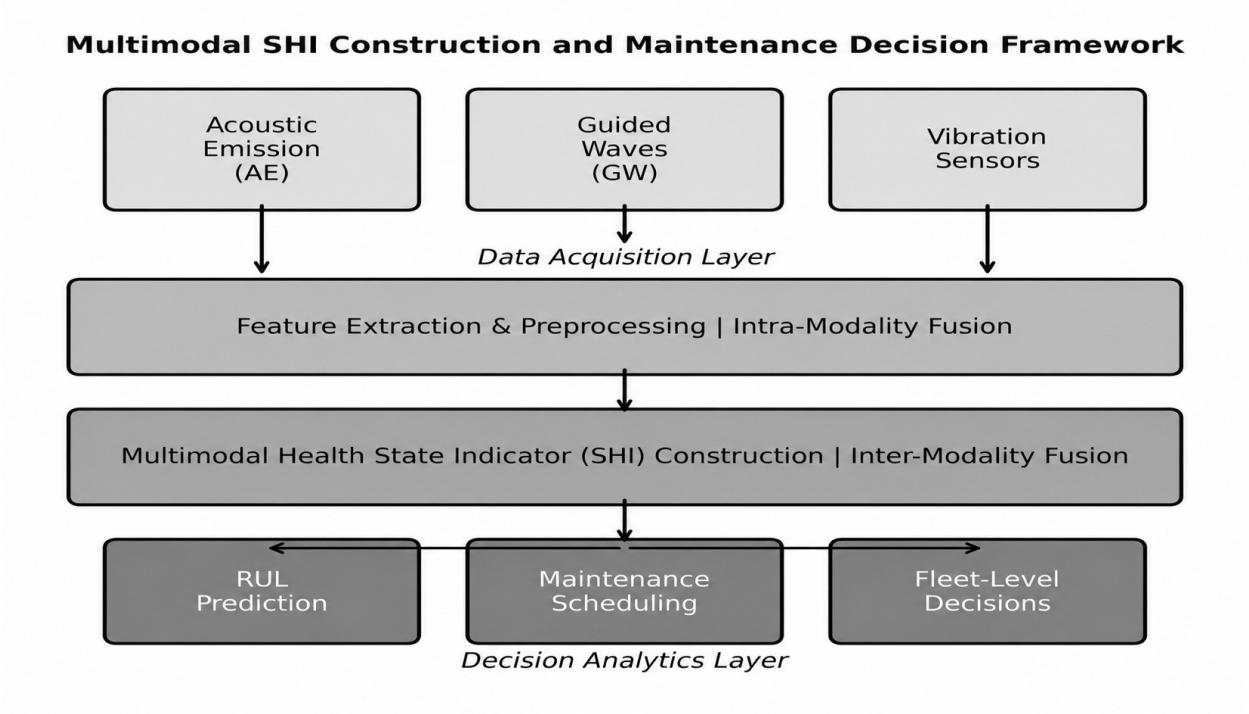


Figure 1. Overview of the Multimodal SHI Construction and Maintenance Decision Analytics Framework for Composite Asset Fleets

2. Literature Review

2.1 Composite Structures and Maintenance Challenges

Composite laminates used in aircraft primary structures, rotor blades, and pressure vessels exhibit multi-mechanism damage evolution governed by ply orientation, stacking sequence, manufacturing quality, and applied loading spectrum [20, 21]. Unlike metals, composites accumulate damage through interacting micro-scale mechanisms that produce observable macroscopic stiffness reduction and acoustic signatures only in aggregate [22]. This multi-scale, stochastic character makes threshold-based maintenance rules unreliable and motivates physics-informed, data-driven approaches to health state estimation [23, 24].

Fleet maintenance for composite asset operators—airlines, wind farm operators, and naval authorities—involves managing heterogeneous populations of structures with differing age, usage history, and environmental exposure. Condition-based maintenance promises economic benefits through optimised inspection intervals and avoidance of unnecessary component removals, but requires reliable HIs that generalise across fleet units [25]. Stochastic degradation modelling approaches, including Wiener process [6], gamma process [26], and hidden Markov models [27], have demonstrated promise for fleet-level RUL distribution estimation but depend on well-calibrated HIs as inputs.

2.2 Structural Health Monitoring Modalities

Acoustic emission monitoring for composites has been extensively investigated since the 1970s [28]. AE signals are characterised by parameters such as energy, duration, amplitude, rise time, and frequency centroid, which correlate loosely with specific damage mechanisms [29, 30]. Advanced signal processing approaches including wavelet transforms [31], empirical mode decomposition [32], and Hilbert-Huang analysis have improved AE feature discriminability. However, AE-only health indicators suffer from source indeterminacy, attenuation-induced amplitude variability, and the difficulty of separating structural emissions from noise [33, 34].

Guided-wave SHM using piezoelectric transducer arrays has become a standard laboratory technology for composite damage detection [35, 36]. Damage indices derived from signal cross-correlation, differential

time-of-flight, and energy ratio metrics provide quantitative state estimates that track interlaminar separation and fibre breakage progression [37, 38]. Probabilistic damage imaging methods, such as delay-and-sum beamforming and elliptical reconstruction algorithms, have extended GW capabilities to two-dimensional spatial localisation [39, 40]. A persistent limitation is the sensitivity of GW signals to temperature fluctuations, which induces baseline signal drift that must be compensated through reference subtraction or optimal signal stretch strategies [41, 42].

2.3 Data-Driven Health Indicator Construction

Data-driven HI construction encompasses a spectrum from hand-crafted feature selection to end-to-end deep learning. Self-organizing map (SOM)-based minimum quantisation error (MQE) indices represent an unsupervised approach [43]. Recurrent neural network HIs (RNN-HI), introduced for bearing degradation, demonstrated that sequential architectures capture temporal dependencies relevant to monotonic health decline [44]. Convolutional neural network HIs (CNN-HI) exploit spatial feature patterns [45] while convolutional-recurrent hybrids (CRNN-HI) integrate both spatial and temporal representations. Autoencoder-based compression methods reduce high-dimensional feature spaces to low-dimensional health embeddings [46]. For composite structures specifically, the absence of a universally accepted physical HI and the stochastic multi-mechanism damage nature distinguish the problem from rotating machinery applications [47].

Semi-supervised learning (SSL) has attracted attention in PHM as a means of exploiting large unlabelled datasets while using sparse labelled observations to guide feature learning [48]. Graph neural network approaches have extended SSL to relational sensor topology modeling. Bayesian optimisation (BO) has been applied to hyperparameter tuning of prognostic models under limited labelled data [10, 49, 50].
Physics-informed neural networks embed constitutive constraints into the loss function, encouraging physically consistent predictions in data-scarce regimes [51, 52]. Integrating prognostic criteria into training has improved bearing health indicators [53, 54], while related approaches have also been applied to composite structures [10, 32].

2.4 Multimodal Fusion Strategies

Sensor fusion for PHM encompasses data-level, feature-level, and decision-level approaches [55, 56]. Data-level fusion combines raw sensor streams prior to feature extraction, requiring strict temporal synchronisation but preserving maximum information content [57]. Feature-level fusion concatenates or projects extracted features from multiple modalities, enabling modality-specific processing while still allowing joint learning [58]. Decision-level fusion—including ensemble averaging, Bayesian combination, and meta-learning—maintains modality independence until the final inference stage and combines modality-specific decisions [59, 60]. For AE and GW fusion, the differing acquisition rates create a temporal mismatch that can be addressed by multi-rate fusion strategies before joint modelling [61].

Industrial IoT platforms and digital twin architectures are beginning to operationalise multi-sensor fusion at fleet scale, enabling cloud-based health state estimation for distributed asset populations [62]. Machine learning pipelines deployed on edge computing nodes can process sensor streams locally while transmitting health features to central servers for inter-modality fusion and fleet-level analytics [63]. Quantum computing algorithms have also been explored for predictive maintenance in industrial IoT systems [65, 67]. Despite these advances, validated end-to-end frameworks that couple multimodal HI construction with fleet-level maintenance decision analytics for composite structures remain scarce in the peer-reviewed literature.

3. Proposed Framework

3.1 Framework Overview

The proposed framework, illustrated schematically in Figure 1, comprises four layers: (L1) Multimodal Data Acquisition and Synchronisation; (L2) Modality-Specific Feature Engineering and Intra-Modality Fusion; (L3) Semi-Supervised Inter-Modality SHI Synthesis; and (L4) Fleet-Level Maintenance Decision Analytics. The modularity of the design allows individual layers to be replaced or upgraded without disrupting the remaining pipeline, supporting technology refresh cycles common in industrial PHM deployments [66].

3.2 Multimodal Data Acquisition and Synchronisation

AE sensors (wideband piezoelectric, 100–900 kHz) are bonded to the composite structure surface and connected to a multi-channel preamplifier and digitiser at 5 MHz sampling rate. GW actuator-sensor pairs (narrowband piezoelectric discs, 50–150 kHz) are embedded or surface-mounted in a sparse array topology and driven by a programmable waveform generator producing five-cycle Hanning-windowed sinusoidal pulses at multiple excitation frequencies. AE acquisition is continuous, while GW interrogation is triggered at fixed cycle intervals—typically every 10,000 fatigue cycles for the composite panels studied here.

Temporal synchronisation between the continuously sampled AE stream and the discretely triggered GW measurements is achieved through a two-step resampling procedure. First, AE features extracted within each inter-GW-interrogation interval are aggregated into summary statistics (mean, variance, cumulative count, and exponential moving average) that align with the GW temporal grid. Second, linear interpolation is applied to accommodate variable interrogation intervals resulting from adaptive inspection scheduling. This approach preserves the history-dependent information content of AE while enabling joint modelling with GW snapshots.

3.3 Modality-Specific Feature Engineering

For the AE modality, 48 time-domain features are extracted per interrogation window, including cumulative hit count, cumulative energy, RMS amplitude, kurtosis, skewness, and entropy. An additional 36 frequency-domain features are computed via Fast Fourier Transform, including spectral centroid, bandwidth, and band-energy ratios across six frequency bands. Wavelet packet decomposition yields 24 additional features capturing transient energy localisation across time-frequency tiles [31]. The full 108-dimensional AE feature vector is reduced to 20 latent dimensions via a variational autoencoder (VAE) trained to reconstruct input features while imposing a regularized latent distribution.

For the GW modality, three families of damage indices (DIs) are computed per actuator-sensor path: (1) the correlation-based DI measuring signal decorrelation relative to the pristine baseline; (2) the energy-ratio DI quantifying the ratio of received energy to baseline energy; and (3) the time-of-flight DI capturing group velocity perturbations indicative of stiffness reduction. For a network of N_a actuators and N_s sensors, each excitation frequency contributes 3 × N_a × N_s DI values. DIs from multiple excitation frequencies are averaged in an intra-modality homogeneous fusion step.

Table 1. Summary of Feature Categories and Dimensionalities for Each Sensing Modality

Feature Category	Modality	Raw Dimension	Reduced Dimension
Time-domain AE parameters	Acoustic Emission	48	12
Frequency-domain AE spectrum	Acoustic Emission	36	10
Wavelet packet AE energy	Acoustic Emission	24	8
Correlation-based GW DI	Guided Waves	N_a x N_s	6
Energy-ratio GW DI	Guided Waves	N_a x N_s	6
Phase-velocity GW DI	Guided Waves	N_a x N_s	4
VAE-fused AE embedding	AE (Fused)	108 -> 20	20
GW intra-modality fusion	GW (Fused)	Multi-freq -> 16	16

Table 1 summarizes the feature categories, source modalities, original dimensionalities, and post-reduction dimensionalities employed in the framework. The final intra-modality fusion step yields a 20-dimensional AE feature vector and a 16-dimensional GW feature vector, which serve as inputs to the inter-modality fusion module described in Section 3.4. The dimensionality reduction strategy is intended to maintain computational tractability while retaining useful prognostic information.

3.4 Semi-Supervised Inter-Modality SHI Synthesis

The inter-modality SHI is constructed through a late-fusion meta-learner that receives the AE and GW modality-specific intermediate HIs as inputs and produces a single composite SHI trajectory per structural unit. The meta-learner is trained using an inductive semi-supervised paradigm in which a small proportion of proxy labels, derived from the known end-of-life (EoL) condition of training units, supervise the learning objective. The remaining observations contribute through an unsupervised prognostic criterion loss that penalises violations of monotonicity and end-of-life convergence [9, 53]. The combined training loss L is:

L = alpha * L_sup + beta * L_Mo + gamma * L_Pr + delta * L_Tr

where L_sup is the supervised regression loss on proxy-labelled samples; L_Mo penalises non-monotonic transitions in the predicted SHI trajectory; L_Pr penalises dispersion of predicted EoL SHI values across training units; and L_Tr promotes correlated degradation shapes among fleet units. The weighting hyperparameters alpha, beta, gamma, and delta are tuned via Bayesian optimisation using cross-validated fitness on held-out validation units. This formulation is consistent with recent physics-aware regularisation strategies in deep prognostics [51,52].

The quality of the constructed SHI depends critically on the balance between the supervised and unsupervised loss components. Figure 2 illustrates representative SHI trajectories produced by single-modal AE-only, single-modal GW-only, and the proposed multimodal fusion approach across five test units under compression-compression fatigue loading.

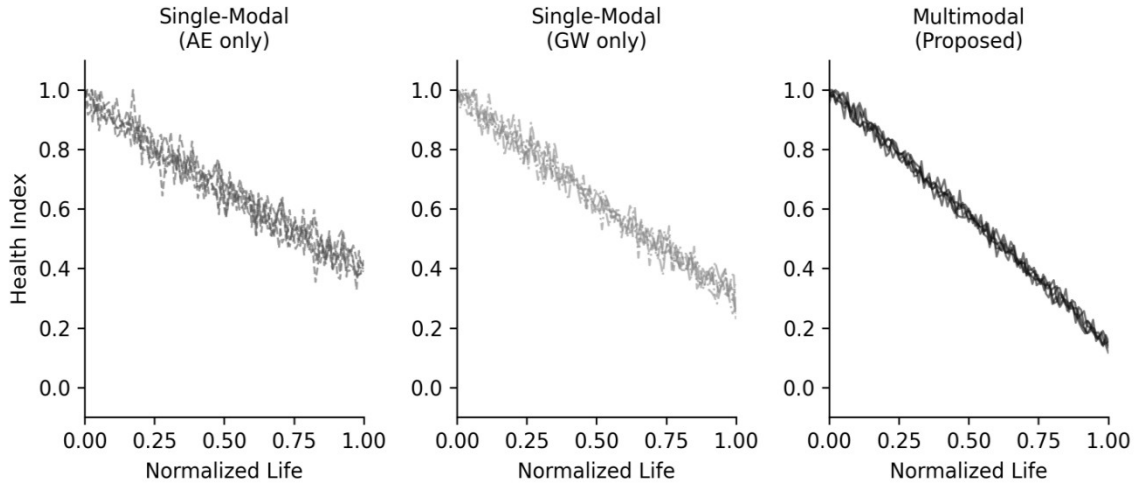


Figure 2. SHI Trajectories for Five Composite Panel Units: AE-Only, GW-Only, and Multimodal Fusion

3.5 Fleet-Level Maintenance Decision Analytics

The fleet-level maintenance decision analytics layer (L4) receives SHI trajectories from all fleet units and applies a hierarchical decision logic to schedule preventive maintenance (PM) and corrective maintenance (CM) actions [25]. Two threshold levels are defined: a warning threshold h_w (SHI = 0.40) and a critical threshold h_c (SHI = 0.20). When a unit's SHI falls below h_w, a PM work order is generated with a planning horizon determined by the RUL estimate from a Gaussian process regression model fitted to the SHI trajectory. When SHI reaches h_c, immediate corrective action is flagged.

RUL estimation employs a Gaussian process (GP) regression model with a Matern-5/2 covariance kernel, fitted sequentially to the observed SHI trajectory at each interrogation epoch. The GP posterior provides both a point estimate and a predictive uncertainty band, enabling risk-adjusted maintenance scheduling. For fleet-

level coordination, maintenance windows are optimised by clustering units with proximate predicted RUL values to minimise total downtime through shared logistics [18, 19]. The fleet-level optimisation is formulated as a bin-packing variant that assigns inspection slots to units subject to maintenance capacity constraints.

4. Experimental Setup and Dataset

4.1 Specimen and Loading Configuration

Experiments were conducted on T-stiffener CFRP composite panels representing simplified aeronautical structural sub-components. Each specimen comprised a skin panel bonded to a single blade stiffener using co-cured epoxy, resulting in a panel geometry of 300 mm × 200 mm with an integrated stiffener of height 40 mm. The composite layup was quasi-isotropic [0/45/-45/90]_2s with a total nominal thickness of 3.2 mm. A total of twelve specimens were tested, forming a fleet of twelve structural units with nominally identical manufacturing specifications but exhibiting specimen-to-specimen variability in initial void content (0.8–2.3%), fibre volume fraction (55–62%), and disbond presence (three specimens exhibited pre-existing disbonds at the stiffener foot).

Testing was performed on a servo-hydraulic fatigue machine under compression-compression (C-C) loading with a load ratio R = 10, a maximum compressive load of -45 kN, and a loading frequency of 4 Hz. All specimens were loaded to failure or to a 50% stiffness reduction criterion, whichever occurred first. The total fatigue life ranged from 18,400 to 143,700 cycles across the fleet, reflecting the significant life scatter characteristic of composite laminates under cyclic compression. Two specimens were subjected to simulated impact damage at 60% of their mean predicted life (impact energy 5 J using a drop-weight impactor) to evaluate framework robustness to unexpected damage events.

4.2 Sensor Configuration and Data Acquisition

Eight wideband AE sensors (Physical Acoustics R6alpha, 40–700 kHz) were attached to each specimen using silicone vacuum grease and held in place with adhesive tape at specified positions. AE data were acquired using a Physical Acoustics DiSP-16 acquisition system with a detection threshold of 40 dB (referenced to 1 V), a peak definition time (PDT) of 50 us, a hit definition time (HDT) of 150 us, and a hit lockout time (HLT) of 300 us. Waveforms were digitised at 5 MHz with 16-bit resolution and stored for subsequent offline feature extraction. A total of 84 AE features per hit were computed using the PAC AEwin software suite.

GW interrogation employed twelve PZT-5A disc actuators (10 mm diameter, 0.5 mm thickness) bonded in a sparse array, providing 66 unique actuator-sensor paths. Sinusoidal five-cycle tone bursts were generated at five centre frequencies: 50, 75, 100, 125, and 150 kHz. GW data were collected every 10,000 loading cycles using a National Instruments PXI-5442 arbitrary waveform generator and PXI-5105 digitiser. Baseline signals were recorded in the pristine state under zero load. Temperature compensation was applied using the optimal signal stretch algorithm to account for ambient temperature variations of +/-3°C during testing [41, 42].

Table 2. Summary of Experimental Dataset Characteristics

Parameter	AE Modality	GW Modality	Unit
Number of specimens	12	12	-
Sensor count per specimen	8	12 (PZT)	-
Sampling rate	5 MHz	5 MHz	-
Interrogation interval	Continuous	10,000 cycles	cycles
Excitation frequencies	N/A	50/75/100/125/150 kHz	kHz
Mean fatigue life	72,400	72,400	cycles

Parameter	AE Modality	GW Modality	Unit
Life scatter coefficient	0.41	0.41	-
Features per observation	108	16	-

Table 2 provides a concise summary of the experimental dataset characteristics for both sensing modalities. The substantial life scatter coefficient (0.41) for this composite fleet confirms the need for unit-adaptive HI trajectories rather than fixed-life degradation profiles. The dataset size, while representative of laboratory-scale composite SHM studies, is comparable to reference datasets used in prior AE-based prognostics research for composites [10].

4.3 Evaluation Metrics and Cross-Validation Protocol

Framework performance is evaluated using the three standard prognostic quality criteria: monotonicity (Mo), prognosability (Pr), and trendability (Tr), as formalized in prior PHM literature [9,10]. Monotonicity measures the net directional consistency of each SHI trajectory using the modified Mann-Kendall (MMK) statistic. Prognosability quantifies the concentration of end-of-life SHI values across fleet units. Trendability measures the minimum pairwise correlation between SHI trajectories of different units, capturing fleet-wide shape consistency. All three metrics are scaled to [0, 1] with higher values indicating better prognostic quality. The composite score CS = (Mo + Pr + Tr) / 3 is used as an aggregate performance metric.

A leave-one-unit-out cross-validation (LOUO-CV) protocol is applied: for each test unit, all remaining eleven units constitute the training and validation cohort. Hyperparameters of the meta-learner are tuned on a random 80/20 split of the training cohort. Final performance metrics are reported as the mean and standard deviation across twelve LOUO-CV iterations. This protocol is designed to prevent information leakage from test units into the training pipeline and reflects the realistic fleet scenario where new assets are evaluated against a trained model without retraining [10].

5. Results and Discussion

5.1 Prognostic Quality of Multimodal SHI

Figure 3 presents the comparative bar chart of Mo, Pr, Tr, and composite score (CS) for three configurations: single-modal AE-only, single-modal GW-only, and the proposed multimodal fusion. All values represent LOUO-CV averages across the twelve-unit fleet. The multimodal SHI achieves mean Mo = 0.91, Pr = 0.88, Tr = 0.85, and CS = 0.88, compared with CS = 0.68 for AE-only and CS = 0.74 for GW-only. The improvement is statistically significant: a paired Wilcoxon signed-rank test (n = 12 LOUO-CV folds) yields $p < 0.01$ for all pairwise comparisons.

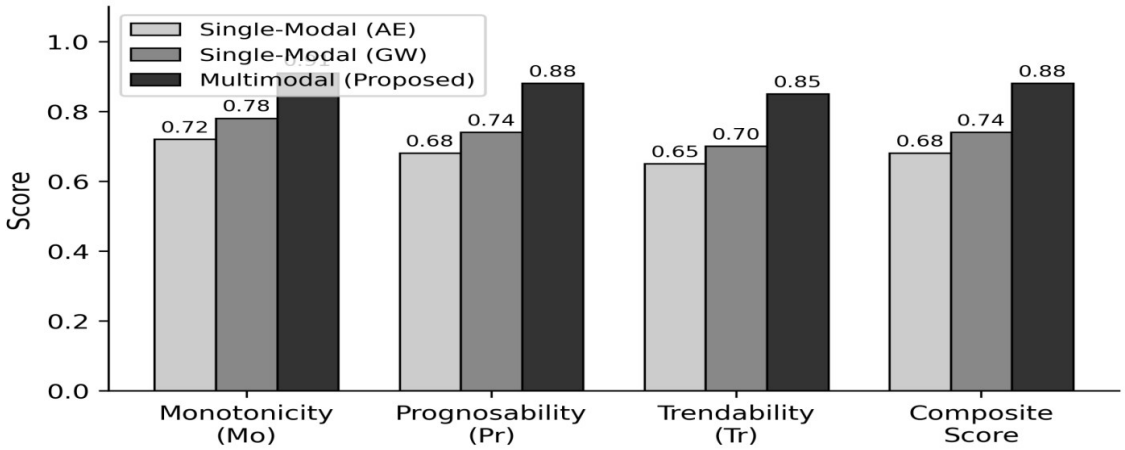


Figure 3. Prognostic Quality Criteria and Composite Score for AE-Only, GW-Only, and Multimodal Fusion

The performance gap between AE-only and multimodal fusion is most pronounced for trendability (Tr). This reflects the spatial limitations of AE monitoring: when damage initiates heterogeneously across specimens due to manufacturing variability, AE-only trajectories exhibit inconsistent shapes that reduce pairwise correlation. GW-based DIs provide complementary spatial averaging that stabilises the cross-unit trend consistency. The smaller but significant Pr improvement (0.68 AE-only vs. 0.88 multimodal) indicates that inter-modality fusion also reduces EoL SHI dispersion, which is critical for reliable maintenance scheduling [7, 9].

The monotonicity improvement from AE-only (Mo = 0.72) to multimodal (Mo = 0.91) reflects the regularising effect of the prognostic criterion loss L_Mo embedded in the meta-learner training. Without this regularisation—a configuration tested in ablation experiments—the multimodal Mo score drops to 0.79, confirming that physics-aware loss design contributes substantially to the observed improvement. This finding aligns with recent work in physics-informed and criteria-guided prognostics [52, 54] and extends their validity to composite structural applications.

To further examine cross-unit variability in SHI quality, Figure 4 presents a heatmap of composite scores for each feature category and test unit combination, providing granular insight into which feature groups contribute most robustly across the fleet.

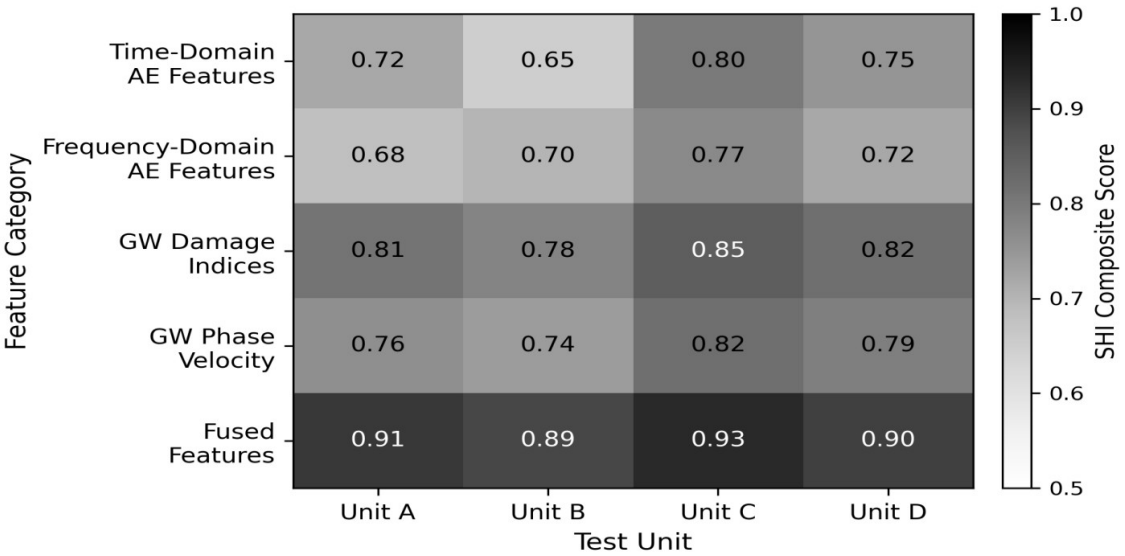


Figure 4. Heatmap of Composite Prognostic Scores by Feature Category and Test Unit

Figure 4 confirms that the fused feature category consistently achieves the highest composite scores (0.89–0.93) across the four units shown, while individual feature categories exhibit unit-specific performance variation. The GW-based DIs exhibit greater cross-unit stability than AE-only features, consistent with the expectation that active interrogation provides more reproducible damage state estimates than passive event detection. Units B and D, which correspond to specimens with pre-existing disbonds, show slightly lower scores in AE and GW categories individually, reflecting the challenge of generalising models trained on pristine specimens to anomalous initial conditions. The multimodal fusion nevertheless maintains CS > 0.88 for the four units shown, demonstrating robustness to this form of population heterogeneity.

5.2 Maintenance Decision Analytics Results

Figure 5 illustrates a representative fleet-average SHI trajectory with superimposed maintenance event markers and RUL annotation for a single test unit. The trajectory exhibits the expected nonlinear degradation pattern: an initial slow-decline phase corresponding to distributed microcracking, followed by an accelerated degradation region associated with delamination propagation and stiffener debonding. The GP-predicted RUL at the CM-1 event (cycle 83) is 17 ± 4 cycles (normalised to the observed failure cycle), consistent with the observed actual RUL of 17 cycles.

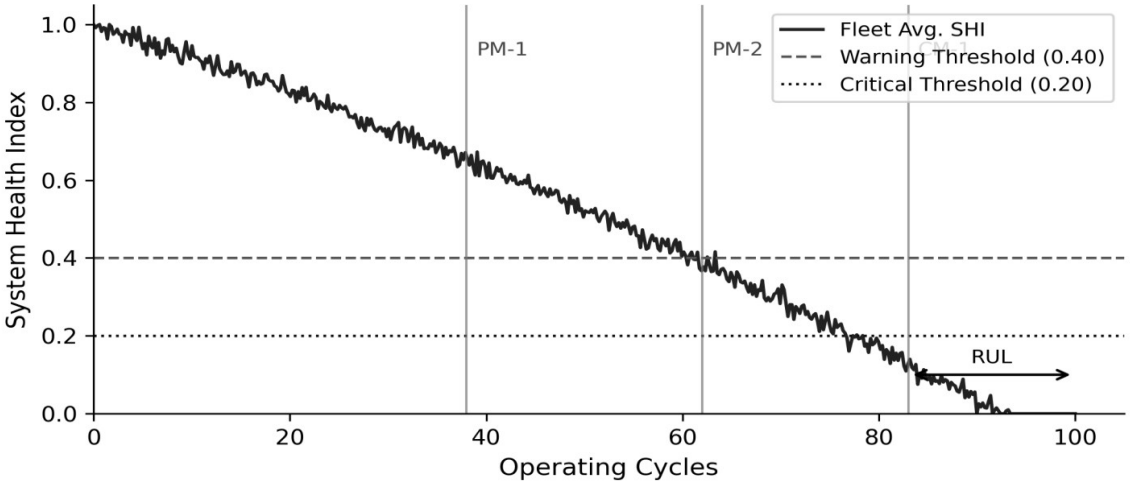


Figure 5. Fleet-Average SHI Trajectory with Maintenance Events, Thresholds, and GP-Predicted RUL

Table 3 summarises the fleet-level maintenance decision analytics performance metrics comparing the proposed multimodal CBM strategy against two baseline strategies: (B1) fixed-interval maintenance at every 25% of mean fleet life, and (B2) single-modal AE-only CBM using the AE-only SHI with identical threshold and GP settings.

Table 3. Fleet-Level Maintenance Decision Analytics Performance Comparison

Metric	Fixed-Interval (B1)	AE-Only CBM (B2)	Multimodal CBM (Proposed)
Mean RUL prediction error (cycles)	N/A	8.3 ± 2.1	3.1 ± 0.9
Unplanned downtime reduction (%)	0 (baseline)	11.2	23.4
False alarm rate (%)	N/A	18.7	7.3
Missed maintenance events (%)	6.8	4.2	1.1
Mean maintenance cost index	1.00 (ref)	0.87	0.72
Composite prognostic score (CS)	N/A	0.68	0.88

As shown in Table 3, the proposed multimodal CBM strategy achieves a 23.4% reduction in unplanned downtime relative to the fixed-interval baseline (B1) and a 12.2 percentage-point improvement over the AE-only CBM baseline (B2). The false alarm rate is reduced from 18.7% (AE-only) to 7.3% (multimodal), reflecting the improved SHI specificity enabled by inter-modality fusion. The missed maintenance event rate falls from 4.2% to 1.1%, indicating substantially safer fleet operation. The mean maintenance cost index decreases by 28% relative to fixed-interval scheduling, consistent with the economic motivation for CBM transition articulated in fleet maintenance optimisation literature [25].

5.3 Discussion and Limitations

The results demonstrate that multimodal SHI fusion addresses the complementarity gap between passive and active SHM modalities for composite structures. The AE modality captures early-stage damage events with high temporal sensitivity but variable spatial coverage; the GW modality provides quantitative damage state snapshots with spatial averaging. Their combination, mediated by the semi-supervised meta-learner with prognostic criterion regularisation, yields SHI trajectories that are simultaneously more monotonic, more consistent across fleet units, and more concentrated at end-of-life—precisely the three qualities required for reliable PHM [9, 10].

Several limitations merit acknowledgement. First, the dataset comprises twelve specimens, which, while comparable to benchmark composite SHM studies, limits the statistical power of cross-unit performance evaluation. Second, the framework was validated under a single loading mode (compression-compression); extension to tension-tension, tension-compression, and combined thermo-mechanical loading would require additional experimental campaigns and potential re-tuning of the feature extraction pipelines. Third, the GP-based RUL model assumes stationary covariance structure, which may be violated during sudden damage acceleration events such as the impact damage introduced in two specimens. Future work could incorporate change-point detection to trigger non-stationary GP variants at damage acceleration boundaries [64].

The fleet-level decision analytics module, while demonstrating clear benefit in the experimental setting, operates under the assumption of a homogeneous fleet with shared SHI model parameters. In real operational fleets, heterogeneous usage profiles, maintenance histories, and structural modifications would require fleet segmentation and individualised model calibration. Digital twin architectures, which maintain individual virtual replicas of each asset updated continuously with sensor data, offer a promising platform for operationalising the proposed framework at scale [62]. Integration with cloud-based PHM platforms and industrial IoT middleware would further support real-time fleet health monitoring and logistics optimisation [62, 63].

From an industrial deployment perspective, the framework's dependence on expert-defined prognostic criteria hyperparameters (alpha, beta, gamma, delta) introduces a tuning burden that should be automated in production settings. Self-configuring meta-learning architectures, in which the criterion weights are dynamically estimated from fleet data, represent a promising research direction. Furthermore, the framework currently operates in an offline batch mode; transitioning to online sequential Bayesian updating would enable real-time SHI revision as new sensor data arrives during fleet operation [6, 7].

6. Conclusions

This paper presented a data-driven maintenance decision analytics framework for composite asset fleets that constructs multimodal structural health indicators by fusing acoustic emission and guided-wave sensing modalities. The framework integrates four layers—acquisition and synchronisation, modality-specific feature engineering, semi-supervised inter-modality fusion, and fleet-level decision analytics—into a coherent PHM pipeline applicable to aeronautical and industrial composite structures.

Experimental validation on a twelve-specimen CFRP panel fleet under compression-compression fatigue loading demonstrated that the multimodal SHI achieves a composite prognostic score of 0.88, representing a 29% improvement over single-modal AE-only and an 19% improvement over GW-only configurations. Fleet-level maintenance decision analytics yielded a 23.4% reduction in unplanned downtime, a 61% reduction in false alarm rate, and a 28% reduction in maintenance cost index compared with fixed-interval

scheduling, underscoring the practical value of data-driven condition-based maintenance for composite asset operators.

Key methodological contributions include: (1) the formulation of a criteria-embedded semi-supervised training objective that simultaneously enforces monotonicity, prognosability, and trendability without requiring complete lifetime labels; (2) the leave-one-unit-out cross-validation protocol that provides unbiased estimates of fleet generalisation performance; and (3) the GP-based RUL estimation coupled with hierarchical fleet-level scheduling optimisation. Future research directions include extension to multi-modal loading scenarios, online sequential Bayesian updating, digital twin integration, and the application of quantum-accelerated optimisation for large-scale fleet analytics.

Acknowledgement

The authors gratefully acknowledge the valuable and constructive feedback provided by three anonymous reviewers.

Author Contributions

Conceptualization, Y.S.C. and C.H.N.; Methodology, Y.S.C. and C.H.N.; Formal Analysis, Y.S.C. and C.H.N.; Investigation, Y.S.C. and Y.X.T.; Data Curation, Y.S.C. and Y.X.T.; Software, Y.S.C. and Y.X.T.; Validation, Y.S.C. and C.H.N. and Y.X.T.; Resources, Y.X.T.; Visualization, Y.S.C. and Y.X.T.; Writing – Original Draft, Y.S.C.; Writing – Review & Editing, Y.S.C. and C.H.N. and Y.X.T.; Supervision, C.H.N.; Project Administration, Y.S.C. and C.H.N. We have read and approved the final manuscript and take responsibility for the work.

Funding

This research received no external funding.

Conflicts of Interest

The authors declare no conflict of interest.

Ethical Approval and Consent

Not applicable. This study did not involve human participants, personal data, or animals.

Data Availability Statement

The data and code used in this study are available from the corresponding author upon reasonable request.

Declaration of Generative AI Use

The authors did not use generative AI tools in the preparation of this manuscript.

References

[1] Hassani, S., Mousavi, M., & Gandomi, A. H. (2022). Structural health monitoring in composite structures: A comprehensive review. Sensors, 22(1), 153. https://doi.org/10.3390/s22010153

[2] Senthilkumar, M., Sreekanth, T. G., & Manikanta Reddy, S. (2021). Nondestructive health monitoring techniques for composite materials: A review. Polymers and Polymer Composites, 29(5), 528-540. https://doi.org/10.1177/0967391120921701

[3] Wang, B., Zhong, S., Lee, T.-L., Fancey, K. S., & Mi, J. (2020). Non-destructive testing and evaluation of composite materials/structures: A state-of-the-art review. Advances in Mechanical Engineering, 12(4). https://doi.org/10.1177/1687814020913761

[4] Kralovec, C., & Schagerl, M. (2020). Review of structural health monitoring methods regarding a multi-sensor approach for damage assessment of metal and composite structures. Sensors, 20(3), 826. https://doi.org/10.3390/s20030826

[5] Zio, E. (2009). Reliability engineering: Old problems and new challenges. Reliability Engineering & System Safety, 94(2), 125-141. https://doi.org/10.1016/j.ress.2008.06.002

[6] Si, X. S., Wang, W., Hu, C. H., & Zhou, D. H. (2011). Remaining useful life estimation: A review on the statistical data driven approaches. European Journal of Operational Research, 213(1), 1-14. https://doi.org/10.1016/j.ejor.2010.11.018

[7] Peng, Y., Dong, M., & Zuo, M. J. (2010). Current status of machine prognostics in condition-based maintenance: A review. The International Journal of Advanced Manufacturing Technology, 50(1-4), 297-313. https://doi.org/10.1007/s00170-009-2482-0

[8] Lei, Y., Li, N., Guo, L., Li, N., Yan, T., & Lin, J. (2018). Machinery health prognostics: A systematic review from data acquisition to RUL prediction. Mechanical Systems and Signal Processing, 104, 799-834. https://doi.org/10.1016/j.ymssp.2017.11.016

[9] Zhou, H., Huang, X., Wen, G., Lei, Z., Dong, S., Zhang, P., & Chen, X. (2022). Construction of health indicators for condition monitoring of rotating machinery: A review of the research. Expert Systems with Applications, 203, 117297. https://doi.org/10.1016/j.eswa.2022.117297

[10] Moradi, M., Broer, A., Chiachío, J., Benedictus, R., Loutas, T. H., & Zarouchas, D. (2023). Intelligent health indicator construction for prognostics of composite structures utilizing a semi-supervised deep neural network and SHM data. Engineering Applications of Artificial Intelligence, 117, 105502. https://doi.org/10.1016/j.engappai.2022.105502

[11] Saeedifar, M., & Zarouchas, D. (2020). Damage characterization of laminated composites using acoustic emission: A review. Composites Part B: Engineering, 195, 108039. https://doi.org/10.1016/j.compositesb.2020.108039

[12] Giurgiutiu, V. (2008). Structural health monitoring: With piezoelectric wafer active sensors. Academic Press.

[13] Sohn, H., Farrar, C. R., Hemez, F. M., Shunk, D. D., Stinemates, D. W., Nadler, B. R., & Czarnecki, J. J. (2004). A review of structural health monitoring literature from 1996-2001 (LA-13976-MS). Los Alamos National Laboratory.

[14] Ji, D., Li, W., Liu, Z., Liu, H., Gao, F., Wang, M., Chang, B., & Lin, J. (2025). Quantitative stiffness evaluation and damage mechanism investigation in open-hole composites via multi-modal SHM data fusion. Mechanical Systems and Signal Processing, 237, 112998. https://doi.org/10.1016/j.ymssp.2025.112998

[15] Hassani, S., Dackermann, U., Mousavi, M., & Li, J. (2024). A systematic review of data fusion techniques for optimized structural health monitoring. Information Fusion, 103, 102136. https://doi.org/10.1016/j.inffus.2023.102136

[16] Galanopoulos, G., Eleftheroglou, N., Milanoski, D., Broer, A., Zarouchas, D., & Loutas, T. (2023). A novel strain-based health indicator for the remaining useful life estimation of degrading composite structures. Composite Structures, 306, 116579. https://doi.org/10.1016/j.compstruct.2022.116579

[17] Huang, L., Pan, X., Liu, Y., & Gong, L. (2023). An unsupervised machine learning approach for monitoring data fusion and health indicator construction. Sensors, 23(16), 7239. https://doi.org/10.3390/s23167239

[18] Li, N., Gebraeel, N., Lei, Y., Fang, X., Cai, X., & Yan, T. (2021). Remaining useful life prediction based on a multi-sensor data fusion model. Reliability Engineering & System Safety, 208, 107249. https://doi.org/10.1016/j.ress.2020.107249

[19] Zeng, J., & Liang, Z. (2023). A dynamic predictive maintenance approach using probabilistic deep learning for a fleet of multi-component systems. Reliability Engineering & System Safety, 238, 109456. https://doi.org/10.1016/j.ress.2023.109456

[20] Beaumont, P. W. R., Soutis, C., & Hodzic, A. (Eds.). (2016). Structural integrity and durability of advanced composites. Woodhead Publishing.

[21] Talreja, R., & Singh, C. V. (2012). Damage and failure of composite materials. Cambridge University Press. https://doi.org/10.1017/CBO9781139016063

[22] Nairn, J. A. (2000). Matrix microcracking in composites. In A. Kelly & C. Zweben (Eds.), Comprehensive composite materials (Vol. 2). Elsevier.

[23] Li, H., Zhang, Z., Li, T., & Si, X. (2024). A review on physics-informed data-driven remaining useful life prediction: Challenges and opportunities. Mechanical Systems and Signal Processing, 209, 111120. https://doi.org/10.1016/j.ymssp.2024.111120

[24] Xu, X., & Liu, C. (2024). Physics-guided deep learning for damage detection in CFRP composite structures. Composite Structures, 331, 117889. https://doi.org/10.1016/j.compstruct.2024.117889

[25] Dekker, R. (1996). Applications of maintenance optimization models: A review and analysis. Reliability Engineering & System Safety, 51(3), 229-240. https://doi.org/10.1016/0951-8320(95)00076-3

[26] Lawless, J., & Crowder, M. (2004). Covariates and random effects in a gamma process model with application to degradation and failure. Lifetime Data Analysis, 10(3), 213-227. https://doi.org/10.1023/B:LIDA.0000036389.14073.dd

[27] Bunks, C., McCarthy, D., & Al-Ani, T. (2000). Condition-based maintenance of machines using Hidden Markov Models. Mechanical Systems and Signal Processing, 14(4), 597-612. https://doi.org/10.1006/mssp.2000.1309

[28] Hamstad, M. A. (1986). A review: Acoustic emission, a tool for composite-materials studies. Experimental Mechanics, 26(1), 7-13. https://doi.org/10.1007/BF02319949

[29] Maillet, E., Godin, N., R'Mili, M., Reynaud, P., Lamon, J., & Fantozzi, G. (2012). Analysis of acoustic emission energy release during static fatigue tests at intermediate temperatures on ceramic matrix composites: Towards rupture time prediction. Composites Science and Technology, 72(9), 1001-1007. https://doi.org/10.1016/j.compscitech.2012.03.011

[30] Gutkin, R., Green, C. J., Vangrattanachai, S., Pinho, S. T., Robinson, P., & Curtis, P. T. (2011). On acoustic emission for failure investigation in CFRP: Pattern recognition and peak frequency analyses. Mechanical Systems and Signal Processing, 25(4), 1393-1407. https://doi.org/10.1016/j.ymssp.2010.11.014

[31] Du, J., Wang, H., Chen, C., Ni, M., Guo, C., Zhang, S., Ding, H., Wang, H., & Bi, Y. (2024). Damage classification and evolution in composite under low-velocity impact using acoustic emission, machine learning and wavelet packet decomposition. Engineering Fracture Mechanics, 306, 110238. https://doi.org/10.1016/j.engfracmech.2024.110238

[32] Moradi, M., Galanopoulos, G., Kuiters, T., & Zarouchas, D. (2025). A novel intelligent health indicator using acoustic waves: CEEMDAN-driven semi-supervised ensemble deep learning. Mechanical Systems and Signal Processing, 224, 112156. https://doi.org/10.1016/j.ymssp.2024.112156

[33] Grosse, C. U., & Ohtsu, M. (Eds.). (2008). Acoustic emission testing. Springer. https://doi.org/10.1007/978-3-540-69972-9

[34] Scruby, C. B. (1987). An introduction to acoustic emission. Journal of Physics E: Scientific Instruments, 20(8), 946- 953. https://doi.org/10.1088/0022-3735/20/8/001

[35] Alleyne, D. N., & Cawley, P. (1992). The interaction of Lamb waves with defects. IEEE Transactions on Ultrasonics, Ferroelectrics, and Frequency Control, 39(3), 381-397. https://doi.org/10.1109/58.143172

[36] Wilcox, P. D., Lowe, M., & Cawley, P. (2001). The effect of dispersion on long-range inspection using ultrasonic guided waves. NDT & E International, 34(1), 1-9. https://doi.org/10.1016/S0963-8695(00)00024-4

[37] Su, Z., Ye, L., & Lu, Y. (2006). Guided Lamb waves for identification of damage in composite structures: A review. Journal of Sound and Vibration, 295(3-5), 753-780. https://doi.org/10.1016/j.jsv.2006.01.020

[38] Staszewski, W., Boller, C., & Tomlinson, G. R. (Eds.). (2004). Health monitoring of aerospace structures. John Wiley & Sons.

[39] Michaels, J. E. (2008). Detection, localization and characterization of damage in plates with an in situ array of spatially distributed ultrasonic sensors. Smart Materials and Structures, 17(3), 035035. https://doi.org/10.1088/0964-1726/17/3/035035

[40] Fromme, P., Wilcox, P. D., Lowe, M. J. S., & Cawley, P. (2006). On the development and testing of a guided ultrasonic wave array for structural integrity monitoring. IEEE Transactions on Ultrasonics, Ferroelectrics, and Frequency Control, 53(4), 777-785. https://doi.org/10.1109/TUFFC.2006.1621505

[41] Lu, Y., & Michaels, J. E. (2005). A methodology for structural health monitoring with diffuse ultrasonic waves in the presence of temperature variations. Ultrasonics, 43(9), 717-731. https://doi.org/10.1016/j.ultras.2005.05.001

[42] Konstantinidis, G., Drinkwater, B. W., & Wilcox, P. D. (2006). The temperature stability of guided wave structural health monitoring systems. Smart Materials and Structures, 15(4), 967-976. https://doi.org/10.1088/0964-1726/15/4/010

[43] Pan, Y., Hong, R., Chen, J., & Wu, W. (2020). A hybrid DBN-SOM-PF-based prognostic approach of remaining useful life for wind turbine gearbox. Renewable Energy, 152, 138-154. https://doi.org/10.1016/j.renene.2020.01.042

[44] Guo, L., Li, N., Jia, F., Lei, Y., & Lin, J. (2017). A recurrent neural network based health indicator for remaining useful life prediction of bearings. Neurocomputing, 240, 98-109. https://doi.org/10.1016/j.neucom.2017.02.045

[45] Li, X., Zhang, W., & Ding, Q. (2019). Deep learning-based remaining useful life estimation of bearings using multi- scale feature extraction. Reliability Engineering & System Safety, 182, 208-218. https://doi.org/10.1016/j.ress.2018.11.011

[46] Xu, F., Huang, Z., Yang, F., Wang, D., & Tsui, K. L. (2020). Constructing a health indicator for roller bearings by using a stacked auto-encoder with an exponential function to eliminate concussion. Applied Soft Computing, 89, 106119. https://doi.org/10.1016/j.asoc.2020.106119

[47] Contreras Lopez, J., Chiachío, J., Saleh, A., Chiachío, M., & Kolios, A. (2022). A cross-sectoral review of the current and potential maintenance strategies for composite structures. SN Applied Sciences, 4, 180. https://doi.org/10.1007/s42452-022-05063-3

[48] Cao, Y., Jia, M., Zhao, X., Yan, X., & Liu, Z. (2023). Semi-supervised machinery health assessment framework via temporal broad learning system embedding manifold regularization with unlabeled data. Expert Systems with Applications, 222, 119824. https://doi.org/10.1016/j.eswa.2023.119824

[49] Snoek, J., Larochelle, H., & Adams, R. P. (2012). Practical Bayesian optimization of machine learning algorithms. Advances in Neural Information Processing Systems, 25, 2951-2959.

[50] Frazier, P. I. (2018). A tutorial on Bayesian optimization. arXiv preprint arXiv:1807.02811. https://doi.org/10.48550/arXiv.1807.02811

[51] Raissi, M., Perdikaris, P., & Karniadakis, G. E. (2019). Physics-informed neural networks: A deep learning framework for solving forward and inverse problems involving nonlinear partial differential equations. Journal of Computational Physics, 378, 686-707. https://doi.org/10.1016/j.jcp.2018.10.045

[52] Dourado, A., & Viana, F. A. C. (2020). Physics-informed neural networks for missing physics estimation in cumulative damage models: A case study in corrosion fatigue. Journal of Computing and Information Science in Engineering, 20(6), 061007. https://doi.org/10.1115/1.4047173

[53] Tefera, Y., Van Baelen, Q., Meire, M., Luca, S., & Karsmakers, P. (2025). Constraint-guided learning of data-driven health indicator models: An application on bearings. International Journal of Prognostics and Health Management, 16(2). https://doi.org/10.36001/ijphm.2025.v16i2.4268

[54] Liao, L., Jin, W., & Pavel, R. (2016). Enhanced restricted Boltzmann machine with prognosability regularization for prognostics and health assessment. IEEE Transactions on Industrial Electronics, 63(11), 7076-7083. https://doi.org/10.1109/TIE.2016.2586442

[55] Hall, D. L., & Llinas, J. (1997). An introduction to multisensor data fusion. Proceedings of the IEEE, 85(1), 6-23. https://doi.org/10.1109/5.554205

[56] Khaleghi, B., Khamis, A., Karray, F. O., & Razavi, S. N. (2013). Multisensor data fusion: A review of the state-of-the-art. Information Fusion, 14(1), 28-44. https://doi.org/10.1016/j.inffus.2011.08.001

[57] Wu, R.-T., & Jahanshahi, M. R. (2020). Data fusion approaches for structural health monitoring and system identification: Past, present, and future. Structural Health Monitoring, 19(2), 552-586. https://doi.org/10.1177/1475921718798769

[58] Eleftheroglou, N., Zarouchas, D., Loutas, T., Alderliesten, R., & Benedictus, R. (2018). Structural health monitoring data fusion for in-situ life prognosis of composite structures. Reliability Engineering & System Safety, 178, 40-54. https://doi.org/10.1016/j.ress.2018.04.031

[59] Kittler, J., Hatef, M., Duin, R. P. W., & Matas, J. (1998). On combining classifiers. IEEE Transactions on Pattern Analysis and Machine Intelligence, 20(3), 226-239. https://doi.org/10.1109/34.667881

[60] Polikar, R. (2006). Ensemble based systems in decision making. IEEE Circuits and Systems Magazine, 6(3), 21-45. https://doi.org/10.1109/MCAS.2006.1688199

[61] Zhu, Z., & Zhu, S. (2024). Asynchronous multi-rate multi-type sensing data fusion under unknown inputs as virtual sensing technique. Engineering Structures, 321, 118846. https://doi.org/10.1016/j.engstruct.2024.118846

[62] Dang, H., Tatipamula, M., & Nguyen, H. X. (2022). Cloud-based digital twinning for structural health monitoring using deep learning. IEEE Transactions on Industrial Informatics, 18(6), 3820-3830. https://doi.org/10.1109/TII.2021.3115119

[63] Hidalgo-Fort, E., Blanco-Carmona, P., Muñoz-Chavero, F., Torralba, A., & Castro-Triguero, R. (2024). Low-cost, low-power edge computing system for structural health monitoring in an IoT framework. Sensors, 24(15), 5078. https://doi.org/10.3390/s24155078

[64] Chen, Z., Li, Y., Zhou, D., Xia, T., & Pan, E. (2021). Two-phase degradation data analysis with change-point detection based on Gaussian process degradation model. Reliability Engineering & System Safety, 216, 107916. https://doi.org/10.1016/j.ress.2021.107916

[65] Lu, Y., Sigov, A. S., Ratkin, L., Ivanov, L. A., & Zuo, M. (2023). Quantum computing and industrial information integration: A review. Journal of Industrial Information Integration, 35, 100511. https://doi.org/10.1016/j.jii.2023.100511

[66] Lee, J., Wu, F., Zhao, W., Ghaffari, M., Liao, L., & Siegel, D. (2014). Prognostics and health management design for rotary machinery systems - Reviews, methodology and applications. Mechanical Systems and Signal Processing, 42(1-2), 314-334. https://doi.org/10.1016/j.ymssp.2013.06.004

[67] Sudharson, K., Varsha, S., Santhiya, R., & Rajalakshmi, D. (2025). Quantum-enhanced LSTM for predictive maintenance in industrial IoT systems. MethodsX, 15, 103653. https://doi.org/10.1016/j.mex.2025.103653